

## SURVEY AND SUMMARY

# Non-canonical DNA transcription enzymes and the conservation of two-barrel RNA polymerases

Gwenaël Ruprich-Robert and Pierre Thuriaux\*

CEA, iBiTec-S, Service de Biologie Intégrative et Génétique Moléculaire, Gif-sur-Yvette Cedex, F-91191, France

Received February 5, 2009; Revised and Accepted March 9, 2010

### ABSTRACT

**DNA transcription depends on multimeric RNA polymerases that are exceptionally conserved in all cellular organisms, with an active site region of >500 amino acids mainly harboured by their Rpb1 and Rpb2 subunits. Together with the distantly related eukaryotic RNA-dependent polymerases involved in gene silencing, they form a monophyletic family of ribonucleotide polymerases with a similarly organized active site region based on two double-Ψ barrels. Recent viral and phage genome sequencing have added a surprising variety of putative nucleotide polymerases to this protein family. These proteins have highly divergent subunit composition and amino acid sequences, but always contain eight invariant amino acids forming a universally conserved catalytic site shared by all members of the two-barrel protein family. Moreover, the highly conserved ‘funnel’ and ‘switch 2’ components of the active site region are shared by all putative DNA-dependent RNA polymerases and may thus determine their capacity to transcribe double-stranded DNA templates.**

### INTRODUCTION

Transcription is catalysed by two distinct DNA-dependent RNA polymerases (RNAPs). Monomeric RNAPs, involved in the transcription of mitochondrial, chloroplast and phage genomes, belong to a super-family of ‘right-handed’ DNA and RNA polymerases (1). However, all other genomes are transcribed by a highly conserved family of RNA polymerases, that was discovered 50 years ago in animal cells and has since then been found to operate in all cellular organisms. These enzymes have a remarkably conserved multi-subunit structure which has been investigated in great details in

the bacterial, archaeal and yeast context, and also operate in nucleo-cytoplasmic DNA viruses (2–12). Together with the single-subunit RNA-dependent RNAPs involved in eukaryotic gene silencing, they form a monophyletic family of ‘two-barrel’ RNAPs (13,14), with a common organization based on two double-Ψ barrels structure with an invariant DxDxD Mg<sup>2+</sup>-binding signature.

These cellular and viral DNA-dependent RNAPs share a surprisingly large active site region of ~500 amino acids, which are present in all bacterial, archaeal and eukaryotic lineages investigated so far and must therefore have already characterized the transcription enzyme of their last common unknown ancestor (LUCA). On the other hand, there is mounting evidence that a variety of extra-chromosomal genomes from bacteria and eukaryotes encode proteins with a far more distant kinship to canonical RNAPs, representing less than one-tenth of the active site mentioned above. These proteins have remarkably divergent amino acid sequences, but share a small core of eight amino acids with the transcription and gene-silencing enzymes mentioned above. Moreover, two additional motifs, corresponding to the switch 2 and funnel domains in the yeast and bacterial RNAPs, are present in all putative DNA-dependent RNAPs and in the proven but atypical transcription enzymes of insect Baculoviruses (15). The present survey will discuss these highly conserved elements and the structural and functional diversity of the new members of the ‘two-barrel’ protein family.

### A COMPLEX ACTIVE SITE SHARED BY ALL CELLULAR DNA-DEPENDENT RNAPs

Following early studies on the bacterial (*Thermus aquaticus*) and yeast (RNAP II of *Saccharomyces cerevisiae*) transcription enzymes (3,7), the complete crystal structure of several bacterial, archaeal and yeast DNA-dependent RNAPs has now been determined at an

\*To whom correspondence should be addressed. Email: p.thuriaux@wanadoo.fr

atomic level of resolution (4,5,9,11,16–18). Their strong conservation extends to five subunits (Rpb1, Rpb2, Rpb3, Rpb6 and Rpb11 in the eukaryotic RNAP II nomenclature adopted here) present in all cellular organisms and forming the entire core structure of bacterial RNAPs (Table 1). In addition, the eukaryotic RNAP I, II and III have seven other core subunits (Rpb4, Rpb5, Rpb7, Rpb8, Rpb9, Rpb10 and Rpb12 in the case of RNAP II) which are also orthologous to archaeal subunits (2,4,5,19,20). Finally, several lineages of nucleocytoplasmic DNA viruses encode multi-subunit RNAPs which presumably derive from the eukaryotic RNAP II form (12,21). Their multi-subunit structure systematically includes the two largest subunits, Rpb1 and Rpb2, as well as the Rpb5 subunit which plays a critical role in the organization of the active site region (22). Subunits akin to Rpb3, Rpb6, Rpb8 and Rpb10 also exist in some viral lineages (Table 1).

Sequence alignments based on current genome databases (<http://blast.ncbi.nlm.nih.gov/Blast.cgi>) reveal ~1000 amino acid positions conserved in all archaeal and eukaryotic nuclear RNAPs. Thus, complex RNAPs essentially similar to those of present-day eukaryotes and archaea existed before the ancestral divergence of the archaeal and eukaryotic kingdoms. The spatial distribution of these amino acids is illustrated in Figure 1A for yeast RNAP II. About half of them are also present in bacterial RNAPs, as predicted by inspecting the genome sequences of all bacterial lineages (Supplementary Data S1). They correspond to some 25 discrete domains of the two large subunits, Rpb1 and Rpb2, with some minor contribution of Rpb3, Rpb6 and Rpb11 (Figure 1B and C), and collectively form a very complex active site organized around two catalytic Mg<sup>2+</sup> ions, called MgA and MgB. Each Mg<sup>2+</sup> is harboured by one of the double-Ψ barrels mentioned above (hereafter called barrel A and B), which are connected by a large ‘bridge’ helix and are associated with a complex network of conserved domains (6–9,17).

## YEAST PLASMIDS ENCODE A PUTATIVE CYTOPLASMIC RPB2::RBP1 FUSION

Several budding yeast species are able to direct killer toxins against other yeast species and to resist their own toxin production. Early studies have shown that, in the dairy yeast *Kluyveromyces lactis*, these properties are governed by two small cytoplasmic DNA genomes, pGK11 and pGK12 (23). The evolutionary origin of these cytoplasmic plasmids is quite puzzling. They are apparently restricted to a small number of closely related yeasts (*K. lactis*, *Lachancea kluyveri*, *Pichia acacia* and *P. etschelli*) and are so far unknown in other eukaryotic lineages, including well-characterized yeasts such as *S. cerevisiae* or *Schizosaccharomyces pombe*. In *K. lactis*, pGK11 ensures the production of the yeast toxin and the corresponding toxin resistance mechanism, whereas pGK12 provides cytoplasmic replication and transcription enzymes which are extremely simplified version of their nuclear counterparts (24,25).

One of the pGK12 gene products is a 982 amino acid protein, Orf6, which has not been biochemically characterized so far but clearly corresponds to an Rpb2::Rpb1-like fusion and thus belongs to the cytoplasmic transcription system (24,25). Orf6 presumably derives from some ancestral yeast Rpb1 and Rpb2 (or their RNAP I and RNAP III paralogues), which was followed by a strongly divergent evolution that fused these two genes, deleted about half of their coding sequence and inserted Orf6-specific domains downstream of the N-terminal Rpb2 ‘protrusion’ and at the junction of the Rpb2 and Rpb1 halves, respectively. It was initially thought that the homology of Orf6 to Rpb2 and Rpb1 was restricted to a few amino acids (24,25). However, updated sequence alignments now extend this homology to ~250 amino acids. They correspond to 11 motifs forming about half of the active site shared by all bacterial, archaeal and eukaryotic RNAPs (Figure 2A, Supplementary Data S1).

**Table 1.** Subunit composition of DNA-dependent RNA polymerases

Organisms		Subunit homology											
Eukaryotes	Pol II ( <i>S. cerevisiae</i> )	Rpb1	Rpb2	Rpb3	Rpb4	Rpb5	Rpb6	Rpb7	Rpb8	Rpb9	Rpb10	Rpb11	Rpb12
	Pol I ( <i>S. cerevisiae</i> )	Rpa190	Rpa135	Rpc40	Rpa14	Rpb5	Rpb6	Rpa43	Rpb8	Rpa12	Rpb10	Rpc19	Rpb12
	Pol III ( <i>S. cerevisiae</i> )	Rpc160	Rpc128	Rpc40	Rpc17	Rpb5	Rpb6	Rpc25	Rpb8	Rpc11	Rpb10	Rpc19	Rpb12
Archaea	<i>M. jannaschii</i>	A' + A''	B' + B''	D	F	H	K	E		M/TFS	N	L	P
	<i>S. solfataricus</i>	A' + A''	B	D	F	H	K	E	G	M/TFS	N	L	P
Viruses	ApMV	+	+	+		+	+						
	ASFV	+	+	+		+	+				+		
	EhV	+	+			+	+		+		+		
	Iridoviruses	+	+			+							
	Poxiviruses	Rpo1	Rpo2	+		Rpo22					Rpo30	Rpo7	
Bacteria	Bacteria (e.g. <i>E. coli</i> )	β'	β	α		ω							α
	Cyanobacteria	γ + β'	β	α		ω							α
	Helicobacteria	β::β'		α		ω							α
Yeast plasmids	pGKL2 ( <i>K. lactis</i> )	Rpb2::Rpb1 (Orf6)											

Subunit symbols are as in refs (2,3,7,19). Note that *M. jannaschii* and the other euryarchaea have no G subunit (20). The (+) symbol corresponds to predicted viral subunits, except for poxiviruses, where a specific nomenclature exists for vaccinia (12). The abbreviated species names correspond to *Saccharomyces cerevisiae*, *Methanocaldococcus jannaschii*, *Sulfolobus solfataricus*, *Escherichia coli* and *Kluyveromyces lactis*. ApMV, ASFV and EhV stand for the *Acanthamoeba polyphaga* mimivirus, African swine fever virus and *Emiliana huxleyi* virus, respectively.

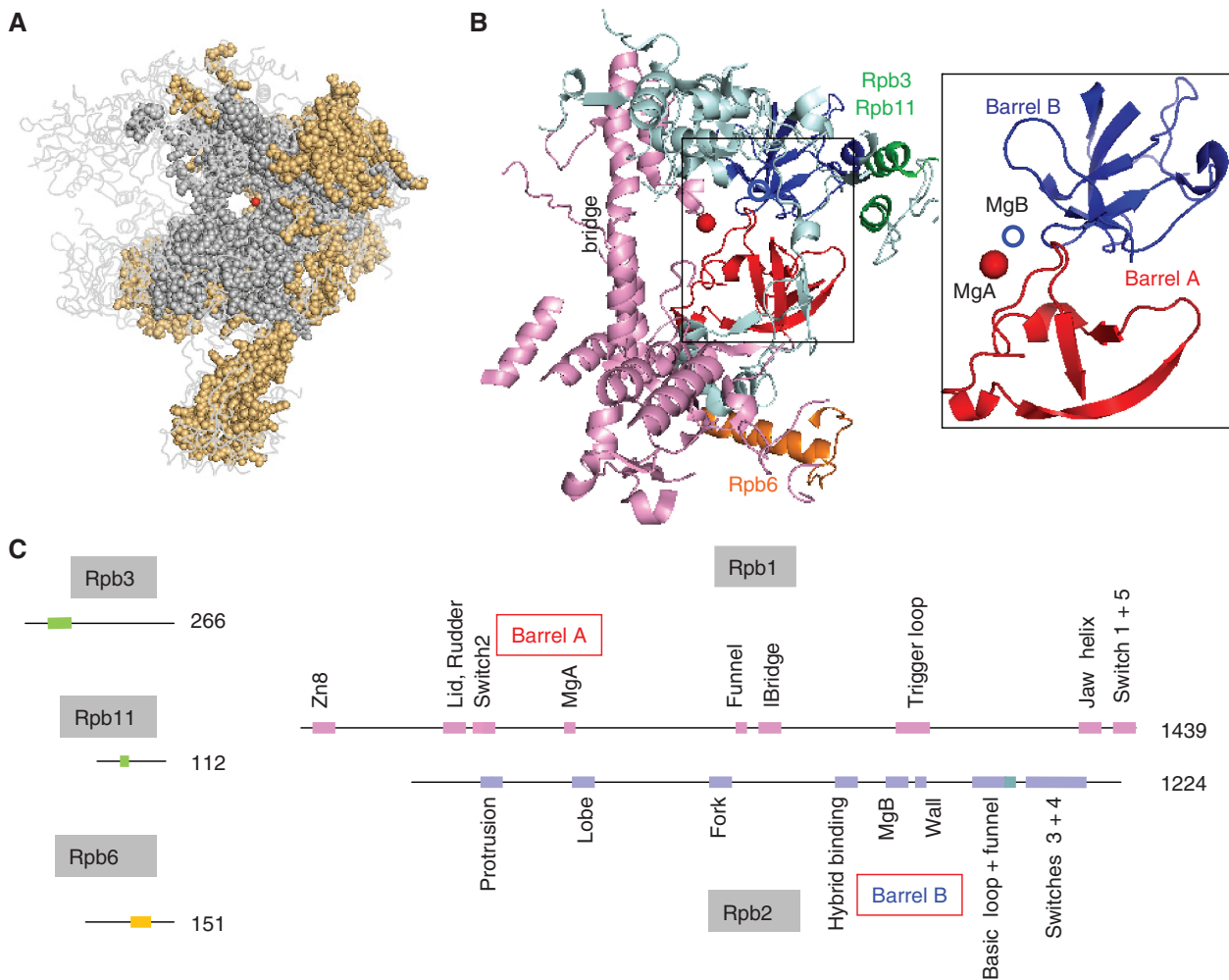


**Figure 1.** Conserved motifs shared by the bacterial, archaeal and eukaryotic RNAPs. (A) Conserved amino acids are shown as grey (all cellular organisms) or orange spheres (archaeal RNAPs and eukaryotic RNAP I, II and III). The red dot denotes the catalytic MgA. This figure corresponds to the sequence alignments provided as Supplementary Data S1 and is based on the 1WCM PDB coordinates showing the complete twelve-subunit-structure of yeast RNAP II (11), using the Pymol software (<http://www.pymol.org>). (B) Spatial organization of the amino acid positions common to all bacterial, archaeal and eukaryotic RNAPs (I, II and III). Experimental data are as in Figure 1A above. Rpb1, Rpb2, Rpb3/11 and Rpb6 domains are in pink, blue, green and orange, respectively. The box illustrates the Barrel A (red) and B (blue) motifs. The corresponding yeast RNAP II positions are 346–365 and 444–487 (Rpb1) and 822–844, 974–1011 and 1074–1089 (Rpb2). (C) Distribution of the corresponding motifs on the Rpb1, Rpb2, Rpb3, Rpb6 and Rpb11 subunits. Colour symbols are as in (B) above. Individual domains are named according to ref. (7), except for part of the Rpb2 hybrid binding domain (positions 964–1028) which is referred to as the basic loop and Rpb2 funnel domains (see text for explanations).

Figure 2B shows the spatial distribution of these conserved domains, as projected on the yeast RNAP II crystal structure. It contains the two double- $\Psi$  barrels mentioned above, connected by the bridge helix and combined with most of the conserved Rpb2 domains also present in the bacterial, archaeal and yeast RNAP II structure. Among them, the protrusion, fork, hybrid binding and switch 3 domains are close to barrel B and surround the RNA/DNA hybrid (Figure 2C). On the other hand, Orf6 has no detectable homology to the highly conserved trigger, switch 1 and switch 5 domains of Rpb1, and also lack the Rpb1 rudder and lid, which form a somewhat less conserved protruding loop domain (6–9,17), suggesting that these domains may not be strictly crucial for transcription, at least in terms of amino acid sequences.

## INSECT DNA VIRUSES ENCODE ATYPICAL RNAPs AND TFIIS FACTORS

Viral multi-subunit RNAPs are typically encoded by nucleo-cytoplasmic large DNA viruses with genomes ranging between ~120 kb (poxviruses) and the 1.2 Mb of the *Amoeba polyphaga* mimivirus (12,21,26). These RNAPs operate during the cytoplasmic phase of their infectious cycle, when the viral DNA is not accessible to the host nuclear transcription system. Other viruses such as the algal Phycodnaviruses have genomes ranging between 185 and 325 kb, but do not reside in their host cytoplasm and are transcribed by their host nuclear transcription system (27). Presumably, this also holds for other large DNA viruses such as the shrimp white spot virus (305 kb) and hypertrophic salivary gland virus of

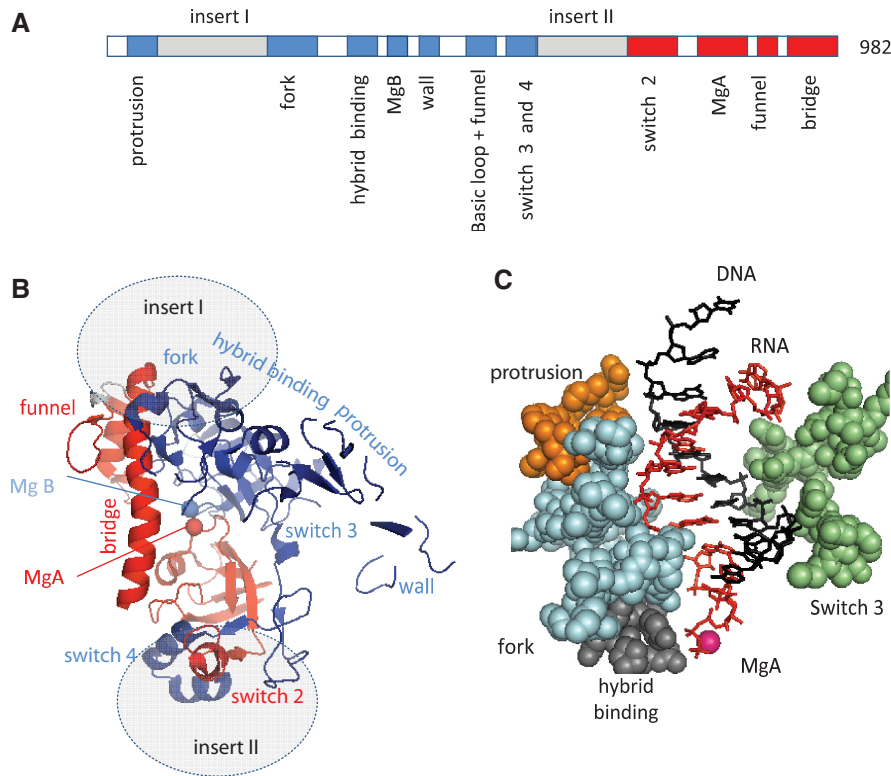


**Figure 2.** Conserved motifs of the Orf6 protein. (A) Distribution of the Orf6-specific (inserts I and II) or Rpb1 (red) and Rpb2 (blue) conserved domains on the Orf6 amino acid chain, based on the sequence alignments provided as Supplementary Data S1. (B) Spatial organization in the yeast RNAP II crystal structure (upper view). This figure is based on the 1R9S PDB coordinates showing the elongating RNAP II (8) using the same colour code and same orientation as in Figure 1B above. Grey ovals denote the hypothetical insertion sites of the Orf6-specific domains. (C) Spatial organization of the conserved protrusion, fork, hybrid binding and switch 3 domains of Rpb2 on each side the RNA/DNA hybrid structure (side view). The orange, blue, grey and green spheres highlight positions 199–210 (protrusion), 466–512 (fork), 763–778 (hybrid binding) and 1106–1131 (switch 3) of yeast Rpb2, respectively. The first nine complementary bases of the RNA and template DNA strand are shown in red and blue, respectively.

*Glossinia pallidipes* (190 kb) which have no RNAP subunit genes (28,29).

The well-characterized insect Baculoviruses, which have DNA genomes of up to 160 kb, do not reside in the cytoplasm of their host, but have an interesting pattern of transcription since a relatively small number of viral genes, specifically expressed during their late infectious cycle, depends on a virus-specific multi-subunit RNAP (15). These enzymes are made of four subunits (called p47, LEF-4, LEF-8 and LEF-9, where LEF stands for late expression factor). They are unrelated to canonical RNAPs, except for a limited similarity of its LEF-9 and LEF-8 subunits to Rpb1 and Rpb2, respectively. Nudiviruses, a sister-group to Baculoviruses, also contain open reading frames weakly but significantly related to the four baculoviral RNAP subunits (30). Moreover, cDNAs encoding the LEF-5 and LEF-8 proteins occur in a library prepared from polydnal viral particles of braconid wasps, which presumably originate from a nudiviral ancestor (31).

The LEF-8 and LEF-9 proteins are therefore restricted to insect viruses, and are themselves rather poorly related between the nudi- and baculoviral lineages. This is best explained by assuming that they originate from eukaryotic Rpb1 and Rpb2 ancestor genes (or of the equivalent

subunits of the other two RNAPs) which underwent a fast and highly divergent evolution obliterating anything that was not strictly needed for DNA transcription. Indeed, a combination of Psi-blast search and visual alignment indicates that their overall similarity to Rpb1 and Rpb2 is limited to ~40 amino acids, which may correspond to a minimal active site region strictly required for the transcription of DNA templates (Figure 3A and Supplementary Data S1). These amino acids belong to the MgA and MgB barrels mentioned above, to the Rpb1 switch 2 domain (positions 329–367 in *S. cerevisiae*) and to a bipartite ‘funnel’ formed by the conserved Rpb1 (746–758) and Rpb2 (1004–1028) motifs near the NTP entry site of yeast RNAP II (8).

Baculoviral transcription also depends on LEF-5, another highly conserved late expression factor which functionally interacts with the viral RNAP (32). LEF-5 has homology with the eukaryotic TFIIS factor associated with RNAP II, RNAP III and perhaps RNAP I (33), with the archaeal TFS, which is akin the eukaryotic subunits Rpa12 (RNAP I) and Rpc11 (RNAP III) and may itself be regarded as a dissociable RNAP subunit (10,34). TFIIS-like factors exist in all lineages of nucleocytoplasmic large DNA viruses investigated so far (Table 1) and are also encoded by Phycodnaviruses (27)

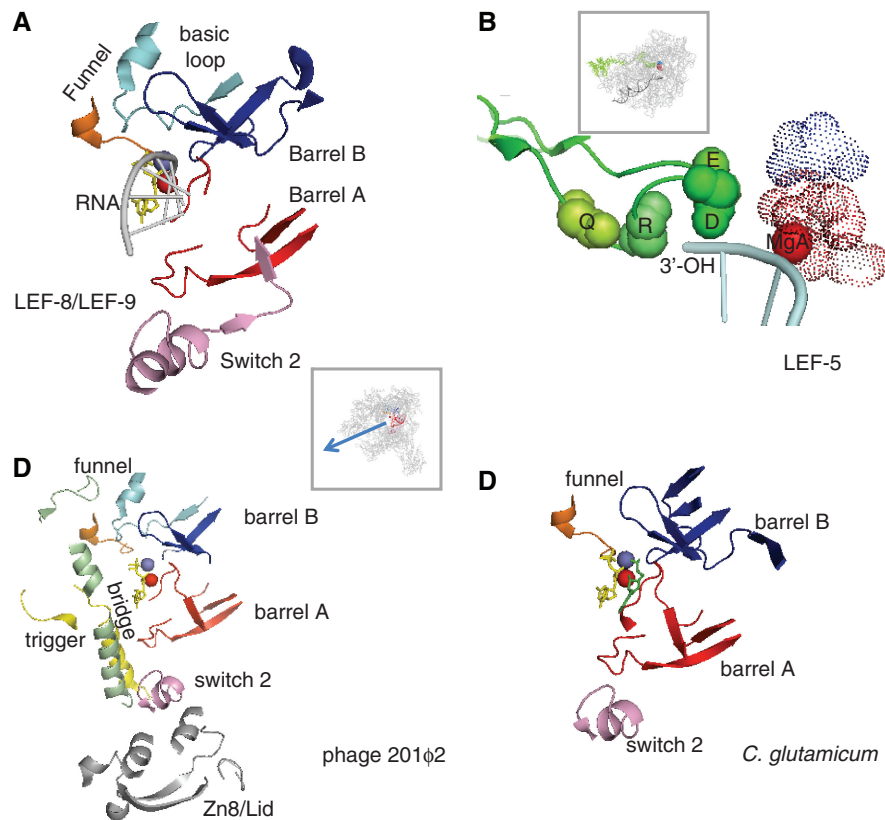


**Figure 3.** Conserved active centre in non-canonical RNAPs. (A) Conserved amino acids in LEF-9/Rpb1 and LEF-8/Rpb2. This figure is based on the 1R9S PDB coordinates which corresponds to the ‘entry’ position incoming NTP (8). Conserved amino acids were as defined in Supplementary Data S1. The Rpb1 and Rpb2 components of the funnel domain are in orange and light blue, respectively. The box shows the entire RNAP II structure in the same spatial orientation. (B) Conserved LeF5/TFIIS C-terminal domain. Four invariant amino acids (Q285, R287, D290 and E291 in the yeast TFIIS) are space-filled (green spheres). The dotted spheres correspond to the invariant carboxylic acids of LEF-9/Rpb1 (D479, D481, D483 of Rpb1, in red) and LEF-8/Rpb2 (D837 of Rpb2, shown in blue). The spatial organization of the corresponding TFIIS, Rpb1 and Rpb2 motifs was taken from the PDB 3GTM2 coordinates which represent RNAP II in its back-tracking conformation (36). The box shows the 10-subunit RNAP II structure in the same spatial orientation. (C) Conserved amino acids in gp275, gp139 and gp273/274 (phage 201 $\phi$ 2). Conserved amino acids were as defined in Supplementary Data S1. This figure is based on the 1R9S PDB coordinates (8), with the same colour code. The bridge, trigger and Zn8/lid domains, which are additionally conserved in gp275, gp130 and gp139 (see Supplementary Data S1) are shown in green, yellow and grey, respectively. Same spatial organization as in (A). (D) Conserved amino acids in NCgl 1702 (*C. glutamicum*). Same spatial organization as in (A).

and by the *G. pallidipes* insect virus (29) which, has mentioned above, lack RNAP subunit genes. Thus, a highly conserved family of TFIIS-like proteins exists in all archaeal, eukaryotic and viral transcription systems, including the atypical late expression transcription of baculo- and nudiviruses. All these proteins share a C-terminal Zn loop with an invariant QxRxxDE motif (Supplementary Data S1), where D and E are immediately close to the catalytic MgA and MgB in a yeast TFIIS/RNAP II binary complex (Figure 3B). This triggers the latent transcript cleavage activity of the RNAP, which removes the backtracked part of the RNA in stalled RNAP molecules and allow them to resume RNA synthesis (35,36).

TFIIS, Rpc11 and the archaeal TFS primarily act as elongation factors, whereas LEF-5 factor appears to be a transcription initiation factor (32), but recent data suggest that yeast TFIIS may be especially critical in a very early phase of the transcription cycle (10). Hence, these factors appear to have a universally conserved role based on the activation of a latent transcript cleavage

activity of their cognate RNAP. Strikingly, the transcript cleavage activity of bacterial RNAPs depends on conserved GreA/B factors present in all bacterial lineages except cyanobacteria. They are unrelated to TFIIS but also contain an invariant GDLxEN signature with two Mg-binding carboxylic acids (37). Intriguingly, they are encoded by the chromosomes of a few Eukaryotes such as *Trichomonas vaginalis* (38), where they presumably result from horizontal gene transfer (Supplementary Data S1).

### ATYPICAL RNAPs MAY ENSURE THE TRANSCRIPTION OF LARGE DNA PHAGES

The transcription of DNA phages usually depends on the host transcription system or on phage-encoded RNAPs similar to the monomeric enzyme of phage T7. However, the recent sequencing of three closely related lytic phages isolated from *Pseudomonas aeruginosa* ( $\phi$ EL,  $\phi$ KZ180) and *P. chlororaphis* (201 $\phi$ 2) has revealed two sets of proteins distantly related to the  $\beta'$  (Rpb1) and  $\beta$  (Rpb2)

subunits of canonical RNAPs (39,40). Mass spectrometry data show that three of them (gp275, gp139 and gp273/724) are present in the 201 $\phi$ 2 virion. The gp275 and gp139 proteins correspond to  $\beta'$ -like N- and C-halves, respectively, whereas gp273/274 is homologous to  $\beta$  for its C-terminal gp274 part, which separated from gp273 separated by a mobile intron. In 201 $\phi$ 2, gp273/274 forms a single band in SDS/polyacrylamide gel electrophoresis, but its two domains may correspond to distinct open reading frames in  $\phi$ EL. A second pair of  $\beta'$ - and  $\beta$ -related proteins corresponds to the gp129 ( $\beta$ -like) and to gp107 ( $\beta'$ -like N-half) and gp130 ( $\beta'$ -like C-half) gene products of 201 $\phi$ 2. They are not detected in the virion and are thus probably expressed upon infection of the bacterial host (39).

These data strongly suggest the existence of two atypical and functionally distinct phage RNAPs (39). Given the lack of  $\alpha$ - or  $\omega$ -like gene products, these transcription enzymes may possibly have a dimeric structure limited to two large subunits. Their amino acid sequences have a limited homology to the canonical  $\beta'$  (Rpb1) and  $\beta$  (Rpb2), and part of this homology corresponds to regions that are specific of the bacterial  $\beta'$  or  $\beta$  subunits (see the sequence alignments shown as Supplementary Data S1). As in the case of the insect baculo- and nudiviruses mentioned above, this is best explained by assuming that these phage proteins derive from bacterial  $\beta'$ - and  $\beta$ -encoding genes which underwent a fast and highly divergent evolution obliterating anything that was not strictly needed for DNA transcription.

In summary, there are now four well-documented examples of proven (Baculoviruses) or putative DNA dependent RNAPs which, as far we can tell, originated from the multi-subunit RNAPs of some some bacterial (*Pseudomonas* phages) or eukaryotic ancestors (insect viruses) and independently evolved towards highly atypical transcription enzymes. Strikingly, the phage enzymes share a common set of  $\sim$ 40 conserved amino acids, that are closely associated in the spatial structure of multi-subunit RNAPs and correspond to the conserved two-barrel, switch 2 and funnel domains also characterizing the LEF-9 and LEF-8 RNAP subunits of the baculo- and nudiviruses (Figure 3C and Supplementary Data S1). As noted below, the latter two domains are absent from RNA-dependent RNA polymerases, thus strongly suggesting that they are strictly critical for the transcription of DNA templates.

$\phi$ EL and  $\phi$ KZ180 have genomes of 211 and 280 kb, respectively, and 201 $\phi$ 2 (317 kb) is actually the largest phage genome sequenced so far (39). This raises the possibility that other long-genome phages, which are notably under-represented in current genome sequences, may have undetected atypical RNAPs. Two pieces of evidence suggest that this is indeed the case. First, the *Bacillus subtilis* phage PBS2 has a poorly characterized RNAP with four polypeptides of 48, 58, 76 and 80 kDa (41), which happen to match the calculated size of the 201 $\phi$ 2 RNAP subunits mentioned above. Second, the *Corynebacterium glutamicum* genome encodes an unusually large (2169 amino acids) NCg1 1702 protein which is distantly related to a  $\beta$ :: $\beta'$  fusion (13). A close inspection

of its amino acid sequence reveals  $\sim$ 40 conserved amino acids, which again correspond to the conserved two-barrel, switch 2 and funnel (Rpb1) domains common to the baculoviral and putative phage RNAPs mentioned above (Figure 3D, Supplementary Data S1). The remaining 98% of NCg11702 bear no obvious relation to any other protein, even in closely related corynebacterial genomes. NCg11702 is therefore an unusually a fast-evolving protein, which may have been recruited to the *C. glutamicum* from an unidentified phage or mobile element.

## PHAGE AND BACTERIAL YONO-LIKE PROTEINS

Single-subunit RNA-dependent RNAPs participate in various forms of RNA-mediated gene silencing in a large range of eukaryotes. Within the same organism, they often coexist under structurally and functionally diverse forms such as the three distinct enzymes of *Neurospora crassa*: Sad1 (involved in meiotic silencing), the poorly characterized Rrp3 protein and Qde1, distantly related to the first two and participating in post-transcriptional gene silencing (14,42). Their homology is chiefly restricted to a bipartite domain of  $\sim$ 60 amino acids, which corresponds to positions 691–747 and 951–1014 of Qde1 and is present in all eukaryotic RNA-dependent RNAPs identified so far (Figure 4A and Supplementary Data S2). As shown in Figure 4B, this bipartite domains forms the most conserved part of the Qde1 two-barrel structure (13).

Iyer *et al.* (13) noted a distant similarity of this bipartite domain to the YonO protein of *B. subtilis* (43), originating from an inserted prophage (SP $\beta$ c2), and a similar open reading frame occurs in the 219 kb DNA genome of the  $\phi$ 8–36 phage of *Bacillus thuringiensis* (44). Our updated Psi-blast search now reveals Yono-like proteins in five different firmicute phages. Moreover, some 50 related proteins are sporadically encountered in the main genomes of firmicutes, cyanobacteria and in two members of the CFB group (*Bacteroides capillosus* and *Bacteroides pectinophilus*). All these proteins have a distant kinship to eukaryotic RNA-dependent RNAPs, but only at the level of the bipartite domain mentioned above, with a common set of eight invariant amino acids that are close to the catalytic MgA in the crystal structure of DNA- and RNA-dependent RNAPs (Figure 4C and D). This strongly argues that these proteins are *bona fide* nucleotide polymerases. On the other hand, their very heterogeneous amino acid sequences (see Supplementary Data S2) indicate a particularly rapid evolution, perhaps associated with phage-mediated lateral gene transfers.

Based on their limited sequence similarity, one may tentatively allocate these proteins to five distantly related families corresponding to the proteins of phages s $\beta$ C2,  $\phi$ 8-36 and 1706, from *B. subtilis*, *B. thuringiensis* and *Lactobacillus lactis*, respectively (43–45), to the cyanobacterial gene products mentioned above and to a single protein encoded by three closely related strains of *B. thuringiensis*. Their distant homology to the eukaryotic RNA-dependent RNAPs suggests a common ancestry,

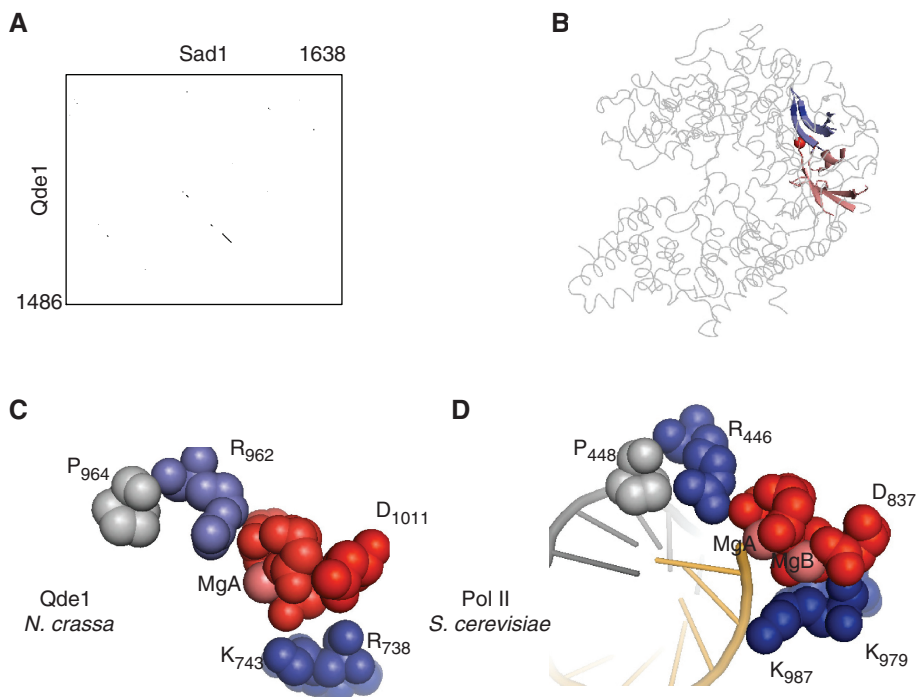


**Figure 4.** A minimal active site shared by all two-barrel RNAPs. (A) Homology of the *Neurospora crassa* RNA-dependent RNAPs (Qde1 and Sad1). The two sequences were aligned by a Blosum 6 matrix at a stringency of 6/23, using the Strider 1.4f6 software (61). (B) Spatial organization of the conserved domain in eukaryotic RNA-dependent RNAPs. This figure is based on the 2J7N PDB coordinates (13). Positions 691–747 (blue) and 955–1014 (red) correspond to the conserved domains shown as in Supplementary Data S2. The less conserved part of the two barrels is in dark grey. The rest of the Qde1 structure, which is poorly conserved, is represented by light grey lines. The red sphere denotes MgA. (C) Blow-up of the eight invariant amino acids shared by all two barrel RNAPs in Qde1 (*N. crassa*). Spheres correspond to MgA, MgB and eight invariant amino acid positions shown in red (D<sub>709</sub>, D<sub>1007</sub>, D<sub>1009</sub> and D<sub>1011</sub>), blue (R<sub>738</sub>, K<sub>743</sub>, R<sub>962</sub>) and grey (P<sub>964</sub>), based on the PDB 2J7N coordinates (14). (D) Blow-up of the eight invariant amino acids shared by all two barrel RNAPs in RNAP II (*S. cerevisiae*). The corresponding invariant positions are Rpb1 D<sub>479</sub>, D<sub>481</sub>, D<sub>483</sub> and Rpb2-D<sub>837</sub> (red), Rpb1-R<sub>446</sub>, Rpb2-K<sub>979</sub> and Rpb2-K<sub>987</sub> (blue) and Rpb1-P<sub>448</sub> (grey), as taken from PDB 1R9T (8).

which may correspond to a very early branch of the two-barrel protein family, that diverged from DNA-dependent RNAPs before the emergence of LUCA and was subsequently lost in Archaea (13). Alternatively, these proteins could have initially originated from DNA-dependent RNAP precursor(s), followed by an extremely divergent evolution associated with the gain of new functions such as RNA amplification or some other form of nucleotide polymerization. This tentatively suggests a role in some RNA-mediated regulation of the corresponding bacterial or (pro)phage genomes. However, such RNA-mediated controls are currently unknown in bacteria, and the biological role of these proteins therefore remains an enigma.

### A HIGHLY CONSERVED CATALYTIC SITE SHARED BY ALL TWO-BARREL RNAPs

All the proteins reviewed in this survey are characterized by eight invariant amino acids located in the immediate vicinity of their catalytic MgA and (when available) MgB cations (Figure 4C and D). This includes the well-characterized Asp (Rpb1<sub>479</sub>DFDGD<sub>483</sub> and Rpb2-D<sub>837</sub> in yeast RNAP II), coordinating the two catalytic Mg<sup>2+</sup>, as well as three basic amino acids (Rpb1-R<sub>446</sub>, Rpb2-K<sub>979</sub>, Rpb2-K<sub>987</sub> in yeast RNAP II), combined with Rpb1-P<sub>448</sub> which presumably defines the precise

position of Rpb1-R<sub>446</sub>. These amino acids have an almost identical spatial distribution in the crystal structure of RNA and DNA-dependent RNAPs. Moreover, site-directed mutagenesis in yeast RNAP II or III have shown that six of these positions are strictly critical *in vivo* (46–48). It should be noted, however, that there is no Rpb1-P<sub>448</sub> mutation available so far, and that the *rpb1-R446A* replacement of yeast RNAP II appears to have no growth defect despite its strict invariance (49).

In keeping with the generic two-metal ions mechanism which probably operates in all nucleotide polymerases (50), studies on yeast and bacterial RNAPs have established that MgA stably resides in the catalytic site, where it is chelated by the Asps of the D.D.D loop and co-ordinates the NTP  $\alpha$ -phosphate and the RNA 3'-OH (5,7,16). MgB, on the other hand, enters with or is stabilized by the incoming NTP. It is co-ordinated by its  $\gamma$ -phosphate and by Rpb1-D<sub>481</sub>, Rpb1-D<sub>483</sub> and Rpb2-D<sub>837</sub> in the yeast RNAP II (8), but occupies a somewhat different position in the bacterial structure of *Thermus thermophilus* (6,17), where it directly interacts with  $\beta'$ -D<sub>739</sub> (equivalent to Rpb1-D<sub>479</sub>) and forms water interactions with  $\beta$ -D<sub>686</sub> (corresponding to Rpb2-D<sub>837</sub>). The Qde1 crystal has no MgB, but the almost identical distribution of its <sub>1007</sub>DYDGD<sub>1011</sub> and D<sub>709</sub> positions leaves little doubt that the eukaryotic RNA-dependent RNAPs and bacterial Yono-like proteins are all

characterized by two catalytic  $Mg^{2+}$ . However, they lack a fifth carboxylic residue (Rpb2-E<sub>836</sub>) present in nearly all other two-barrel RNAPs (Supplementary Data S1) and holding MgB by an additional water-mediated bond (6,17).

Recent X-Rays studies on yeast RNAP II indicate that NTPs are loaded through a pore leading to the active centre (8). It has been suggested that the incoming NTP first binds to an entry (E) site and then rotates around MgB to reach the final nucleotide addition (A) site (8). This provides a rationale for the extreme conservation of three positively charged residues (Rpb1-R<sub>446</sub>, Rpb2-K<sub>979</sub> and Rpb2-K<sub>987</sub>) in the catalytic site. Rpb1-R<sub>446</sub> and the Rpb2-K<sub>979</sub>/Rpb2-K<sub>987</sub> pair occupy the end of this NTP entry pore, on each side of the two  $Mg^{2+}$ , and are immediately close to Rpb1-D<sub>485</sub> and Rpb1-D<sub>483</sub>, respectively. The positively charged side chains of Rpb2-K<sub>979</sub> and Rpb2-K<sub>987</sub> face the last two nucleotides of RNA in the elongating bacterial and yeast RNAPs (7). In the E site, the  $\gamma$ -phosphate of the incoming NTPs is co-ordinated by Rpb2-K<sub>987</sub> and MgB. It then rotates around MgB to reach the A site, which brings its ribose ring close to side chain of Rpb1-R<sub>446</sub> (Figure 5A and B). The precise inter-atomic distance between Rpb2-K<sub>979</sub> and Rpb2-K<sub>987</sub> appears to be highly critical, given the lethality of the yeast *rpb2-K979R* or *rpb2-K987R* mutations (47). Moreover, the *rpoB-K1065R* mutation of *Escherichia coli* (equivalent to *rpb2-K979R*) produces dominant negative effect *in vivo*, with a

mutant RNAP that synthesises dinucleotides but cannot enter elongation (51).

Beyond these eight amino acids, all DNA-dependent two-barrel RNAPs (including the putative RNAPs of *Pseudomonas* phages) share Rpb1-K<sub>332</sub>, on the switch 2 domain, and Rpb1-G<sub>750</sub>, Rpb1-K<sub>752</sub> and Rpb2-R<sub>1020</sub> (forming a salt bridge with Rpb2-D837) on the funnel domain (Figure 5B and C). The switch 2 domain bears several conserved Arg and Lys (including Rpb1-K<sub>332</sub>) which hold the template DNA strand upstream of the catalytic site. Accordingly, the corresponding yeast *rpb1-K332A* and *rpb1-R344A* mutations are highly prone to abortive transcription (49), suggesting a direct role in the formation of the DNA transcription bubble. The funnel domain is located beneath the catalytic site. It forms the most conserved part of the NTP pore mentioned above, and may thus be specifically required to load NTP. Thus, Rpb1-K<sub>752</sub> and Rpb2-R<sub>1020</sub> would delineate the NTP entry site, together with Rpb2-K<sub>987</sub>. This is supported by the fact that RNAP III mutations of the funnel domain (*rpc160-L792S* and *rpc128-V955M*) compensate a temperature-sensitive mutation altering the MgA loop, perhaps by favouring the delivery of NTPs to the catalytic site (52). We note that the funnel structure may be specifically imposed by the double-stranded nature of the RNA template. This would be consistent with the fact that, *in vitro*, yeast RNAP II is also able to transcribe double-stranded RNA templates (53).

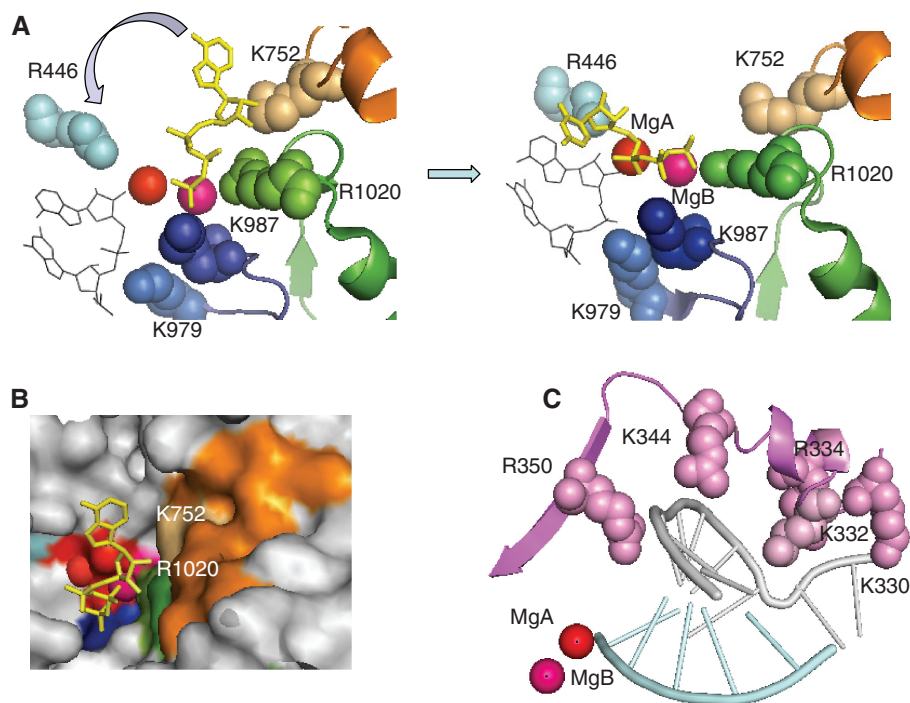


**Figure 5.** NTP loading and organization of the switch 2 domain in yeast RNAP II. (A) NTP loading. The left and right panel correspond to the NTP entry and addition configurations, respectively, and are based on the PDB 1R9T and 1R9S coordinates (8). The invariant Rpb1-R<sub>446</sub> (light blue), the Rpb2-K<sub>979</sub> and Rpb2-K<sub>987</sub> of the basic loop (dark blue), and the Rpb1-K<sub>752</sub> and Rpb2-R<sub>1020</sub> of the funnel domain (orange and green) are shown as space-filled spheres. The red and magenta spheres denote the catalytic MgA and MgB, respectively. The incoming NTP is shown in yellow. Thin black lines indicate the last two nucleotides of the RNA transcript. A blue arrow symbolises the rotation of the NTP toward the 3'-OH end of the transcript. (B) View of the entry site showing the surface of the RNAP II molecule at the end of the secondary channel (NTP entry pore). Same colour code as above, with additional indication of the DFDGD MgA loop. (C) Switch 2 domain: the switch 2 motif (Rpb1<sub>327-351</sub>) is shown in magenta. Space-filled spheres denote positively charged residues. Crystallographic coordinates were taken from PDB 1R9T (8).



## CONCLUSIONS

The diversity of the two-barrel RNAP family is now well documented, as first suggested by Iyer *et al.* (13), and extends far beyond the two main classes of DNA- or RNA-dependent RNAPs. Most of the newly discovered members of this protein super-family are proven (15) or putative non-canonical RNAPs encoded by eukaryotic DNA viruses and bacterial phages (or inserted prophages DNA), which are much under-represented in current databases. Likewise, their apparent lack in the archaeal kingdom could merely reflect our very limited knowledge of archaeal viruses (54). Thus, their real diversity may be greater than currently meet the eyes. Except for the well-characterized DNA-dependent RNAPs of Baculoviruses (15), little is known of their biological role(s), notably in the case of the enigmatic Yono-like proteins or NcG1702 gene product of *C. glutamicum* (13). We have assumed here that they act as nucleotide polymerases, but this evidently calls for direct experimental studies.

All known members of the two-barrel protein family share eight closely spaced amino acids, of which seven have negatively (Asp) or positively charged side chains (Arg, Lys). In DNA-dependent RNAPs, four invariant Asp coordinate two catalytic  $Mg^{2+}$ , whereas the incoming NTP and the growing end of the RNA transcript interact with the  $Mg^{2+}$  ions and with the positively charged side chains of Rpb2-K<sub>979</sub>, Rpb2-K<sub>987</sub> and Rpb1-R<sub>446</sub>. Other positively charged residues, belonging to the switch 2 and funnel domains, are highly conserved or even strictly invariant (Rpb1-K<sub>332</sub>, Rpb1-K<sub>752</sub> and Rpb2-K<sub>1020</sub>) in all cellular or viral DNA-dependent two-barrel RNAPs and thus probably determine the transcription of double-stranded DNA templates. Such combinations of catalytic  $Mg^{2+}$ , Asp, Arg and Lys are not specific of the two-barrel RNAPs, but are a common pattern of other, structurally unrelated families of nucleotide polymerases. All these enzymes probably emerged during the early steps of pre-cellular evolution, but have distinct ways of loading their NTPs and show substantial differences in the architecture of their catalytic domain (6,8,17,55–58).

Unlike the sporadic distribution of the eukaryotic RNA-dependent RNAPs and bacterial Yono-like proteins, multi-subunit DNA-dependent RNAPs operate in all bacterial, archaeal and eukaryotic lineages, with no known exception. Remarkably, these enzymes have an almost invariant core structure of ~500 strongly conserved amino acids, also found in most virus-encoded RNAPs (12,21), in two recently discovered plant RNAPs (59,60) and, to some extent, in the simplified Orf6 protein of yeast ‘killer’ plasmids (24,25). Hence, the LUCA of all cellular organisms must itself have had an elaborated DNA-dependent RNAP with the same complex active site of ~500 amino acids, possibly distributed on several polypeptide subunits. The ulterior evolution of this RNAP thus primarily concerned its DNA recruitment factors (corresponding to bacterial  $\sigma$  subunits or to pre-initiation complexes with a TATA box binding protein in the archaea and eukaryotes), along with the acquisition of

backtracking properties mediated by the bacterial GreA/B or archaeo-eukaryotic TFIS-like factors.

We have seen above that the putative RNAPs encoded by *Pseudomonas* phages have some homology to bacterial-specific  $\beta$  and  $\beta'$  domains and thus presumably derive from bacterial ancestors. Likewise, the insect-specificity of the Baculo- and Nudiviruses argues for a eukaryotic ancestry of their LEF-8 and LEF-9 RNAP subunits. Hence, these proteins are unlikely to be archaic forms of DNA-dependent RNAPs, but probably result from the highly divergent evolution of bacterial and eukaryotic DNA-dependent RNAPs ancestors, which obliterated most of their ~500 strongly conserved positions but retained what was strictly for DNA transcription, including the switch 2 and funnel domains. In sharp contrast to the conserved active site of all cellular and nucleo-cytoplasmic viral RNAP, this implies a largely unconstrained evolution of these atypical phage and viral RNAPs that, moreover, may only be competent for the transcription of a small number of genes (15). It will therefore be interesting to know how far the catalytic properties of these enzymes have diverged from their cellular counterparts in terms of elongation rate, processivity or promoter recognition mechanisms.

## SUPPLEMENTARY DATA

Supplementary Data are available at NAR Online.

## ACKNOWLEDGEMENTS

Part of this article was written whilst one of us (P.T.) was a guest of Dr Austen Ganley and his colleagues at the Institute of Natural Science, Massey University (New Zealand). We also thank Dr Michel Werner for useful comments and discussion.

## FUNDING

French Agence Nationale de la Recherche (grant BLAN08-3-309259). Funding for open access charge: Commissariat à l'énergie atomique and French Agence Nationale de la Recherche (grant BLAN08-3-309259).

*Conflict of interest statement.* None declared.

## REFERENCES

- Cermakian, N., Ikeda, T.M., Miramontes, P., Lang, B.F., Gray, M.W. and Cedergren, R. (1997) On the evolution of the single-subunit RNA polymerases. *J. Mol. Evol.*, **45**, 671–681.
- Werner, F. and Weinzierl, R.O. (2002) A recombinant RNA polymerase II-like enzyme capable of promoter-specific transcription. *Mol. Cell*, **10**, 635–646.
- Zhang, G., Campbell, E.A., Minakhin, L., Richter, C., Severinov, K. and Darst, S.A. (1999) Crystal structure of *Thermus aquaticus* core RNA polymerase at 3.3 Å resolution. *Cell*, **98**, 811–824.
- Korkhin, Y., Unligil, U.M., Littlefield, O., Nelson, P.J., Stuart, D.I., Sigler, P.B., Bell, S.D. and Abrescia, N.G. (2009) Evolution of Complex RNA Polymerases: The Complete Archaeal RNA Polymerase Structure. *PLoS Biol.*, **7**, e102.

5. Hirata, A., Klein, B.J. and Murakami, K.S. (2008) The X-ray crystal structure of RNA polymerase from Archaea. *Nature*, **451**, 851–854.
6. Nudler, E. (2009) RNA polymerase active center: the molecular engine of transcription. *Annu. Rev. Biochem.*, **78**, 335–361.
7. Cramer, P., Bushnell, D.A. and Kornberg, R.D. (2001) Structural basis of transcription: RNA polymerase at 2.8 Å resolution. *Science*, **292**, 1863–1876.
8. Westover, K.D., Bushnell, D.A. and Kornberg, R.D. (2004) Structural basis of transcription: nucleotide selection by rotation in the RNA polymerase II active center. *Cell*, **119**, 481–489.
9. Vassylyev, D.G., Vassylyeva, M.N., Perederina, A., Tahirov, T.H. and Artsimovitch, I. (2007) Structural basis for transcription elongation by bacterial RNA polymerase. *Nature*, **448**, 157–162.
10. Werner, M., Thuriaux, P. and Soutourina, J. (2009) Structure-function analysis of RNA polymerase I and III. *Curr. Opin. Struct. Biol.*, **19**, 740–745.
11. Armache, K.J., Kettenberger, H. and Cramer, P. (2003) Architecture of initiation-competent 12-subunit RNA polymerase II. *Proc. Natl Acad. Sci. USA*, **100**, 6964–6968.
12. Moss, B., An, B.V., Amegadzie, B., Gershon, P.D. and Keck, J.C. (1991) Cytoplasmic transcription system encoded by vaccinia virus. *J. Biol. Chem.*, **266**, 1355–1358.
13. Iyer, L.M., Koonin, E.V. and Aravind, L. (2003) Evolutionary connection between the catalytic subunits of DNA-dependent RNA polymerases and eukaryotic RNA-dependent RNA polymerases and the origin of RNA polymerases. *BMC Struct. Biol.*, **3**, 1.
14. Salgado, P.S., Koivunen, M.R., Makeyev, E.V., Bamford, D.H., Stuart, D.I. and Grimes, J.M. (2006) The structure of an RNAi polymerase links RNA silencing and transcription. *PLoS Biol.*, **4**, e434.
15. Guarino, L.A., Xu, B., Jin, J. and Dong, W. (1998) A virus-encoded RNA polymerase purified from baculovirus-infected cells. *J. Virol.*, **72**, 7985–7991.
16. Bushnell, D.A. and Kornberg, R.D. (2003) Complete, 12-subunit RNA polymerase II at 4.1-Å resolution: implications for the initiation of transcription. *Proc. Natl Acad. Sci. USA*, **100**, 6969–6973.
17. Vassylyev, D.G., Vassylyeva, M.N., Zhang, J., Palangat, M., Artsimovitch, I. and Landick, R. (2007) Structural basis for substrate loading in bacterial RNA polymerase. *Nature*, **448**, 163–168.
18. Spahr, H., Calero, G., Bushnell, D.A. and Kornberg, R.D. (2009) Schizosaccharomyces pombe RNA polymerase II at 3.6-Å resolution. *Proc. Natl Acad. Sci. USA*, **106**, 9185–9190.
19. Langer, D., Hain, J., Thuriaux, P. and Zillig, W. (1995) Transcription in Archaea: similarity to that in Eucarya. *Proc. Natl Acad. Sci. USA*, **92**, 5768–5772.
20. Kwapisz, M., Beckouet, F. and Thuriaux, P. (2008) Early evolution of eukaryotic DNA-dependent RNA polymerases. *Trends Genet.*, **24**, 211–215.
21. Iyer, L.M., Balaji, S., Koonin, E.V. and Aravind, L. (2006) Evolutionary genomics of nucleocytoplasmic large DNA viruses. *Virus Res.*, **117**, 156–184.
22. Zarus, C., Briand, J.F., Bouldar, Y., Labarre-Mariotte, S., Garcia-Lopez, C., Thuriaux, P. and Navarro, F. (2007) Functional organization of the Rpb5 subunit shared by the three yeast RNA polymerases. *Nucleic Acids Res.*, **35**, 634–647.
23. Gunge, N. (1986) linear DNA killer plasmids from the yeast *Kluiveromyces*. *Yeast*, **2**, 152–163.
24. Tommasino, M., Ricci, S. and Galeotti, C.L. (1988) Genome organization of the killer plasmid pGKL2 from *Kluiveromyces lactis*. *Nucleic Acids Res.*, **16**, 5863–5877.
25. Wilson, D.W. and Meacock, P.A. (1988) Extranuclear gene expression in yeast: evidence for a plasmid-encoded RNA polymerase of unique structure. *Nucleic Acids Res.*, **16**, 8097–8112.
26. Raoult, D., Audic, S., Robert, C., Abergel, C., Renesto, P., Ogata, H., La Scola, B., Suzan, M. and Claverie, J.M. (2004) The 1.2-megabase genome sequence of Mimivirus. *Science*, **306**, 1344–1350.
27. Dunigan, D.D., Fitzgerald, L.A. and Van Etten, J.L. (2006) Phycodnaviruses: a peek at genetic diversity. *Virus Res.*, **117**, 119–132.
28. Yang, F., He, J., Xionghui, L., Qin, L., Deng, P., Xiaobo, Z. and Xun, X. (2001) Complete genome sequence of the shrimp white spot bacilliform virus. *J. Virol.*, **75**, 11811–11820.
29. Abd-Alla, A.M., Cousserans, F., Parker, A.G., Jehle, J.A., Parker, N.J., Vlak, J.M., Robinson, A.S. and Bergoin, M. (2008) Genome analysis of a *Glossina pallidipes* salivary gland hypertrophy virus reveals a novel, large, double-stranded circular DNA virus. *J. Virol.*, **82**, 4595–4611.
30. Wang, Y. and Jehle, J.A. (2009) Nudiviruses and other large, double-stranded circular DNA viruses of invertebrates: new insight on an old topic. *J. Invertebrate Pathol.*, **101**, 187–193.
31. Bezier, A., Annaheim, M., Herbinier, J., Wetterwald, C., Gyapay, G., Bernard-Samain, S., Wincker, P., Roditi, I., Heller, M., Belghazi, M. et al. (2009) Polydnnaviruses of braconid wasps derive from an ancestral nudivirus. *Science*, **323**, 926–930.
32. Guarino, L.A., Dong, W. and Jin, J. (2002) In vitro activity of the baculovirus late expression factor LEF-5. *J. Virol.*, **76**, 12663–12675.
33. Ghavi-Helm, Y., Michaut, M., Acker, J., Aude, J., Thuriaux, P., Werner, M. and Soutourina, J. (2008) Genome-wide location analysis reveals a role for TFIIS in RNA polymerase III transcription. *Genes Dev.*, **22**, 1934–1947.
34. Hausner, W., Lange, U. and Musfeldt, M. (2000) Transcription factor S, a cleavage induction factor of the archaeal RNA polymerase. *J. Biol. Chem.*, **275**, 12393–12399.
35. Kettenberger, H., Armache, K.J. and Cramer, P. (2004) Complete RNA polymerase II elongation complex structure and its interactions with NTP and TFIIS. *Mol. Cell*, **16**, 955–965.
36. Wang, D., Bushnell, D.A., Huang, X., Westover, K.D., Levitt, M. and Kornberg, R.D. (2009) Structural basis of transcription: backtracked RNA polymerase II at 3.4 Å resolution. *Science*, **324**, 1203–1206.
37. Opalka, N., Chlenov, M., Chacon, P., Rice, W.J., Wriggers, W. and Darst, S.A. (2003) Structure and function of the transcription elongation factor GreB bound to bacterial RNA polymerase. *Cell*, **114**, 335–345.
38. Carlton, J.M., Hirt, R.P., Silva, J.C., Delcher, A.L., Schatz, M., Zhao, Q., Wortman, J.R., Bidwell, S.L., Alsmark, U.C., Besteiro, S. et al. (2007) Draft genome sequence of the sexually transmitted pathogen *Trichomonas vaginalis*. *Science*, **315**, 207–212.
39. Thomas, J.A., Rolando, M.R., Carroll, C.A., Shen, P.S., Belnap, D.M., Weintraub, S.T., Serwer, P. and Hardies, S.C. (2008) Characterization of *Pseudomonas chlororaphis* myovirus 201varphi2-1 via genomic sequencing, mass spectrometry, and electron microscopy. *Virology*, **376**, 330–338.
40. Hertveldt, K., Lavigne, R., Pleteneva, E., Sernova, N., Kurochkina, L., Korchevskii, R., Robben, J., Mesyanzhinov, V., Krylov, V.N. and Volckaert, G. (2005) Genome comparison of *Pseudomonas aeruginosa* large phages. *J. Mol. Biol.*, **354**, 536–545.
41. Clark, S., Losick, R. and Pero, J. (1974) New RNA polymerase from *Bacillus subtilis* infected with phage PBS2. *Nature*, **252**, 21–24.
42. Shiu, P.K., Raju, N.B., Zickler, D. and Metzberg, R.L. (2001) Meiotic silencing by unpaired DNA. *Cell*, **107**, 905–916.
43. Kunst, F., Ogasawara, N., Moszer, I., Albertini, A.M., Alloni, G., Azevedo, V., Bertero, M.G., Bessieres, P., Bolotin, A., Borchert, S. et al. (1997) The complete genome of the gram-positive bacterium *Bacillus subtilis*. *Nature*, **390**, 249–256.
44. Thomas, J.A., Hardies, S.C., Rolando, M., Hayes, S.J., Lieman, K., Carroll, C.A., Weintraub, S.T. and Serwer, P. (2007) Complete genomic sequence and mass spectrometric analysis of highly diverse, atypical *Bacillus thuringiensis* phage 0305phi8-36. *Virology*, **368**, 405–421.
45. Garneau, J.E., Tremblay, D.M. and Moineau, S. (2008) Characterisation of 1706, a virulent phage from *Lactococcus lactis* with similarities to prophages from other Firmicutes. *Virology*, **373**, 298–309.
46. Dieci, G., Hermann-Le Denmat, S., Lukhtanov, E., Thuriaux, P., Werner, M. and Sentenac, A. (1995) A universally conserved region of the largest subunit participates in the active site of RNA polymerase III. *EMBO J.*, **14**, 3766–3776.
47. Treich, I., Carles, C., Sentenac, A. and Riva, M. (1992) Determination of lysine residues affinity-labeled in the active site

- of yeast RNA polymerase II(B) by mutagenesis. *Nucleic Acids Res.*, **20**, 4721–4725.
48. Langelier, M.F., Baali, D., Trinh, V., Greenblatt, J., Archambault, J. and Coulombe, B. (2005) The highly conserved glutamic acid 791 of Rpb2 is involved in the binding of NTP and Mg(B) in the active center of human RNA polymerase II. *Nucleic Acids Res.*, **33**, 2629–2639.
  49. Majovski, R.C., Khapersky, D.A., Ghazy, M.A. and Ponticelli, A.S. (2005) A functional role for the switch 2 region of yeast RNA polymerase II in transcription start site utilization and abortive initiation. *J. Biol. Chem.*, **280**, 34917–34923.
  50. Steitz, T.A. (1998) A mechanism for all polymerases. *Nature*, **391**, 231–232.
  51. Kashlev, M., Lee, J., Zolenskaya, K., Nikiforov, V. and Goldfarb, A. (1990) Blocking of the initiation-to-elongation transition by a transdominant RNA polymerase mutation. *Science*, **248**, 1006–1009.
  52. Rozenfeld, S. and Thuriaux, P. (2001) A genetic look at the active site of RNA polymerase III. *EMBO Rep.*, **2**, 598–603.
  53. Lehmann, E., Brueckner, F. and Cramer, P. (2007) Molecular Basis of RNA dependent RNA polymerase II activity. *Nature*, **450**, 445–449.
  54. Prangishvili, D., Garrett, R.A. and Koonin, E.V. (2006) Evolutionary genomics of archaeal viruses: unique viral genomes in the third domain of life. *Virus Res.*, **117**, 52–67.
  55. Aravind, L., Mazumder, R., Vasudevan, S. and Koonin, E.V. (2002) Trends in protein evolution inferred from sequence and structure analysis. *Curr. Opin. Struct. Biol.*, **12**, 392–399.
  56. Lescar, J. and Canard, B. (2009) RNA-dependent RNA polymerases from flaviviridae and picornaviridae. *Curr. Opin. Struct. Biol.*, **19**, 759–767.
  57. Delarue, M., Poch, O., Tordo, N., Moras, D. and Argos, P. (1990) An attempt to unify the structure of polymerases. *Prot. Engin.*, **3**, 461–467.
  58. Bruenn, J.A. (2003) A structural and primary sequence comparison of the viral RNA-dependent RNA polymerases. *Nucleic Acids Res.*, **31**, 1821–1829.
  59. Pontier, D., Yahubyan, G., Vega, D., Bulski, A., Saez-Vasquez, J., Hakimi, M.A., Lerbs-Mache, S., Colot, V. and Lagrange, T. (2005) Reinforcement of silencing at transposons and highly repeated sequences requires the concerted action of two distinct RNA polymerases IV in Arabidopsis. *Genes Dev.*, **19**, 2030–2040.
  60. Herr, A.J., Jensen, M.B., Dalmay, T. and Baulcombe, D.C. (2005) RNA polymerase IV directs silencing of endogenous DNA. *Science*, **308**, 118–120.
  61. Marck, C. (1988) “DNA strider”: a C program for the fast analysis of DNA and protein sequences on the Apple Macintosh family of computers. *Nucleic Acids Res.*, **16**, 1829–1836.